Critical slowing down mechanism and reentrant dipole glass phenomena in $(1-x)BaTiO_3$-$xBiScO_3$ ($0.1 \leqslant x \leqslant 0.4$): The high energy density dielectrics

S. S. N. Bharadwaja,* J. R. Kim, H. Ogihara, L. E. Cross, S. Trolier-McKinstry, and C. A. Randall

Center for Dielectric Studies, Materials Research Institute, The Pennsylvania State University, University Park, Pennsylvania 16802, USA

(Received 18 July 2010; published 28 January 2011)

The dielectric and ferroelectric switching properties of high temperature-high energy density $(1-x)BaTiO_3$-$xBiScO_3$ ($0.1 \leqslant x \leqslant 0.4$) dielectrics were investigated over a broad temperature range. It was found that these ceramics possess dipole glass features such as critical slowing down of the dielectric relaxation, polarization hysteresis aging, rejuvenation, and holelike memory below the dipole glass transition temperature (T_{DG}). The dielectric relaxation behavior is consistent with a three-dimensional Ising model with critical slowing exponents $(z\upsilon) = 10 \pm 1$ and composition-dependent glass transition temperatures. At lower temperatures, $(1-x)BaTiO_3$-$xBiScO_3$ ceramics transform into a reentrant dipole glass state owing to the breakup of local polar ordering. A phase diagram is developed marking the paraelectric, ferroelectric, and dipole glass regimes as a function of composition with the reentrant features.

DOI: 10.1103/PhysRevB.83.024106 PACS number(s): 77.80.−e, 81.40.Rs, 64.60.Ht

I. INTRODUCTION

There is a need for high energy density dielectrics ($>1\ J/cm^3$) that can operate above 250 °C for SiC-based power electronic inverters.[1,2] Recent studies on bulk $(1-x)BaTiO_3$-$xBiScO_3$ ($0 < x < 0.5$) ceramics and thin films suggest that these may be candidate materials for this application.[3,4] Ogihara, Randall, and Trolier-McKinstry showed that several $(1-x)BaTiO_3$-$xBiScO_3$ compositions exhibit high permittivity values (~1000) and high, temperature-stable energy storage capabilities (~6 J/cm^3) with breakdown fields exceeding 1 MV/cm.[5] Collectively these properties point to $(1-x)BaTiO_3$-$xBi(Me',Me'')O_3$ materials as having very attractive properties for high energy density ceramic or thin-film capacitors.[6–8]

$BaTiO_3$ is a well-known ferroelectric with a space group $P4mm$ and lattice parameters $a = 3.986$ Å and $c = 4.026$ Å at room temperature.[9] $BiScO_3$ has a monoclinic space group $C2/c$ with $a = 9.889$ Å, $b = 5.822$ Å, $c = 10.046$ Å, and $\beta = 108.3°$.[10] $BiScO_3$ is a distorted perovskite with both oxygen octahedral tilting and antiparallel Bi displacements along the b axis.[10] Neither ferroelectric nor antiferroelectric behavior has been experimentally demonstrated in $BiScO_3$.[11,12] Recent structural studies by an x-ray diffraction (XRD) technique indicated that $(1-x)BaTiO_3$-$xBiScO_3$ ceramics, for $0.05 \leqslant x \leqslant 0.20$, transform gradually from the tetragonal to cubic phase via a region with coexisting tetragonal and rhombohedral phases at room temperature.[13]

Dielectric measurements revealed a gradual change from normal ferroelectric behavior in $BaTiO_3$ to a highly diffuse, relaxorlike behavior for $0.1 \leqslant x \leqslant 0.4$, as shown in Fig. 1. Ogihara, Randall, and Trolier-McKinstry[5] reported a substantial frequency dependence in the dielectric data in $(1-x)BaTiO_3$-$xBiScO_3$ for $0.1 \leqslant x \leqslant 0.5$. This was analyzed using the loss tangent (ω_{max}) maxima within the framework of the Vogel-Fulcher formalism:

$$\omega_{max} = \omega_0 \exp\left[\frac{-E}{k\left(T_{max} - T_f\right)}\right]. \quad (1)$$

The resultant activation energies (E) were between 0.2 and 0.35 eV with attempt frequencies of (ω_0) ~ 10^{12}–10^{13} Hz. The associated freezing temperatures (T_f) increased from ~100 to 165 K with increasing x values. These activation energy values are significantly larger than those of Pb-based [such as $(Pb,La)(Zr,Ti)O_3$ (PLZT) and $Pb(Mg_{1/3}Nb_{2/3})O_3$ (PMN)] or Bi-based perovskite relaxor ferroelectric materials.[14] The origin for the dielectric relaxation was speculated to be owing to a weakly coupled relaxor behavior for $0.1 \leqslant x \leqslant 0.4$.[5] Moreover, a distinct cusp in the remanent polarization versus temperature was noticed at low temperatures, unlike the behavior observed in relaxor ferroelectrics such as PMN, $xBiScO_3$-$yPbTiO_3$-$zPb(Mg_{1/3}Nb_{2/3})O_3$, and $(Sr_xBa_{1-x})Nb_2O_6$.[3,15,16]

A fundamental understanding of relaxor ferroelectricity has been pursued from both experimental and theoretical viewpoints for more than two decades.[17–19] Many of the approaches originated from the magnetic analogs known as spin glasses.[20] It is believed that relaxor ferroelectricity arises from a competition between long-range forces promoting dipole ordering and the breakup of the translational symmetry owing to chemical disorder. As a result, the local random bonds and random fields create ensembles of polar nanoregions (PNRs) and produce the characteristic dielectric relaxation.[21–23] The mechanism responsible for the critical slowing down in the functional properties can differ for different compositions and materials, as the effective Hamiltonian (H) is governed by the cross coupling between polarization states as well as random-field interactions:[24–26]

$$H = \frac{1}{2}\sum_{i,j} K_{ij}\sigma_i\sigma_j - \frac{1}{2}\sum_{i,j} J_{ij}\sigma_i\sigma_j - \sum_i h_i\sigma_i - F\sum_i \sigma_i, \quad (2)$$

where σ_i, σ_i are components of the dimensionless dipole moment field. The summation terms in (1) represent dipolar interactions K_{ij}, random-bond interactions (J_{ij}), random fields (h_i), and the external field (F), respectively.

As shown in Table I, there are a wide range of materials that exhibit relaxation in their functional properties. For example, magnetic spin glasses show dispersion in the magnetic susceptibility linked to frustration in the ordering of magnetic spins, whereas dipole glasses have a frequency-dependent

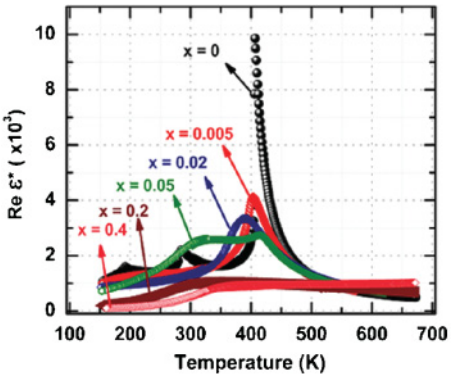

FIG. 1. (Color online) Dielectric permittivity vs temperature in $(1-x)BaTiO_3$-$xBiScO_3$ ceramics for $0.1 \leqslant x \leqslant 0.4$. The measurements were taken at 1 kHz with 1 V_{rms}.

dielectric permittivity. The associated relaxation time scales vary from 10^{-13} to 10^{-6} s. In all the materials listed in Table I, the functional properties are characterized by a shift in their maxima to higher temperatures (T_{max}) with increasing measurement frequency, obeying the Vogel-Fulcher law.[27] One of the characteristic features of spin glasses as well as dipole glasses includes aging in functional properties, with "dip" or "hole"-like memory effects below the spin-glass and/or dipole glass transition temperature (T_{DG}). Below T_{DG}, the functional properties exhibit critical slowing down features governed by time- and frequency-dependent scaling effects.[28] In spin glasses, *weak* anisotropy in random fields with random exchange fields can cause local ordering, and as a result a switchable magnetization will be developed below the freezing temperature.[29–31] In most spin glasses and relaxor ferroelectrics, the magnitude of the switchable magnetization and/or polarization continues to rise as the temperature falls. However, in *reentrant spin glasses*, at low enough temperatures ($T<T_{DG}$), the ability to field induce spin ordering is lost owing to large random dipolar interactions. As a result, the ferromagnetic phase transforms into a nonergodic spin-glass state. Thus, reentrant spin glasses are distinguishable from canonical spin glasses based on high-field switching measurements in which a rise in switchable magnetization occurs before it drops below the spin-glass transition temperature. Examples of magnetic reentrant spin glasses are known in the literature (e.g., $NiGa_2S_4$, $Dy_xY_{1-x}Al_2$).[28,29] with detailed experimental evidence showing the disappearance of high-field ferromagnetic switchable magnetization at low temperatures. However, in the dielectric analog dipole glass literature, reentrant behavior was suggested as a possible mechanism for the underlying dielectric relaxation phenomena in compounds such as K(Ta,Nb)O_3 (Ref. 32) and $Pb(Mg_{1/3}Nb_{2/3})O_3$-$PbTiO_3$

TABLE I. Classes of materials that exhibit relaxation in their functional properties.

Type	Relaxation feature	Examples	References
Glass	Supercooled liquids having a broad distribution of relaxation time constants	Borosilicates	36
Spin glass	Relaxation in the magnetic susceptibility is owing to the interaction between random fields and random exchange fields.	AuMn, dilute magnets	28
Cluster glass	Relaxation in the magnetic susceptibility is owing to the presence of a critical concentration of dopants that form clusters of spins.	AuMn alloys	37, 38
Strain glass	Dispersive strain versus frequency responses	Ti-Ni alloys	39
Dipole glass	Relaxation in the dielectric permittivity is owing to defect dipoles or off-centered ions in incipient ferroelectric materials.	$K(Nb_xTa_{1-x})O_3$	40, 41
		Li-$KTaO_3$	
Proton glass	Dielectric relaxation is owing to deuteration of hydrogen-bonded ferroelectrics and/or (dis)ordering of O-H-O bonds.	$Rb_{1-x}(NH_4)_xH_2PO_4$ type	42
Quadrupole glass	The dielectric relaxation results from hydrogen occupying either an ortho position or a para position.	Organic liquids	43
Orientational glass	Owing to spatial orientation of defect dipoles and/or rotators	Liquid crystals, canted spin magnets	31 31
Relaxor ferroelectrics	Dynamic polar nanoregions arise from an optical soft mode. A frequency-dependent permittivity develops as a result of dynamic polar nanodomains.	PMN	26, 27, 44, 45, 46
		$(Sr,Ba)NbO_6$	
		$(Pb,La)(Zr,Ti)O_3$	
		$BiScO_3$-$Pb(Mg_{1/3}Nb_{2/3})O_3$-$PbTiO_3$	
Reentrant spin glass	*Weak* anisotropic random fields interact with random exchange fields to create short-range ordering. As a result, a reentrant ferromagnetic state with switchable magnetization appears between the ergodic and nonergodic spin-glass states.	$NiGa_2S_4$; $Dy_xY_{1-x}Al_2$; amorphous dilute magnets	28,29

(Refs. 33 and 34) type single crystals and/or ceramics with little confirmation of disappearance of switchable polarization under high-field experiments at low temperatures.

The goal of this paper is to probe the mechanism of dielectric relaxation in the bismuth scandate–barium titanate solid solution in more detail. The high apparent activation energies in $(1-x)BaTiO_3$-$xBiScO_3$ suggest[5] that there may be significant differences in the origin of the dielectric relaxation relative to canonical relaxor ferroelectrics. To explore these features further, the temperature and frequency dependence of the dielectric and ferroelectric properties of $(1-x)BaTiO_3$-$xBiScO_3$ ($0.1 < x < 0.5$) ceramics were examined in this work. The *dipole glass* behavior is evident from critical slowing down features below the dipolar glass transition temperatures (T_{DG}). In addition, characteristic phenomena such as aging, memory, and rejuvenation effects[35] were analyzed for the $x = 0.3$ composition. Low-temperature switching measurements showed a drop in the remanent polarization values for $0.1 \leqslant x \leqslant 0.4$, below a critical temperature, suggesting that this solid solution acts as a reentrant dipole glass.

II. EXPERIMENTAL PROCEDURE

Homogenous and single-phase $(1-x)BaTiO_3$-$xBiScO_3$ powders were prepared for $0.1 < x < 0.4$ by a solid-state reaction route, as described elsewhere,[3] using reagent grade $BaCO_3$ (99.0%, Alfa Aesar), TiO_2 (99.97%, 0.25 μm, Ishihara), Bi_2O_3 (99.9%, MCP), and Sc_2O_3 (99.0%, The Low Hanging Fruit Company). The calcined powders were mixed with organic binders, dispersants, and solvents in a slurry that was tape cast under a doctor blade. Single dielectric layer ($\sim$27 μm thick and 13.3 mm^2 area) capacitors were formed by laminating tapes with screen-printed platinum inks for inner electrodes. The binders were removed and the ceramics were sintered. Finally, end termination electrodes were applied to enable electrical characterization. The details of the capacitor processing can be found elsewhere.[5] XRD studies using a Scintag Pad V diffractometer with Cu$K\alpha$ radiation (35 kV, 30 mA, 0.6 s/step) confirmed the perovskite phase of the samples. As reported previously, the samples were single phase up to $x \leqslant 0.4$; for higher $BiScO_3$ concentrations, the samples exhibited mixed phases.[5]

Dielectric and ferroelectric measurements were performed from 100 to 600 K in Delta Design chambers at constant heating or cooling rates (-0.5 to -3 K/min). An impedance analyzer (HP4192A) was utilized to measure the dielectric properties over a frequency range of 100 Hz to 1 MHz, with an oscillating voltage of 1.0 V_{rms}. Temperature-dependent polarization-electric field switching measurements were done in a virtual ground mode in a cryogenic probe station (model TTP6, LakeShore Cryotronics, Inc., Westerville, OH) in conjunction with a temperature controller (model 332, LakeShore Cryotronics, Inc.). The dielectric and ferroelectric properties were compared under zero-field conditions as a function of composition. In addition, dipole glass features such as aging, rejuvenation, and memory were examined.

III. RESULTS AND DISCUSSION

Figure 2 shows the real and imaginary components of the dielectric permittivity as a function of temperature for

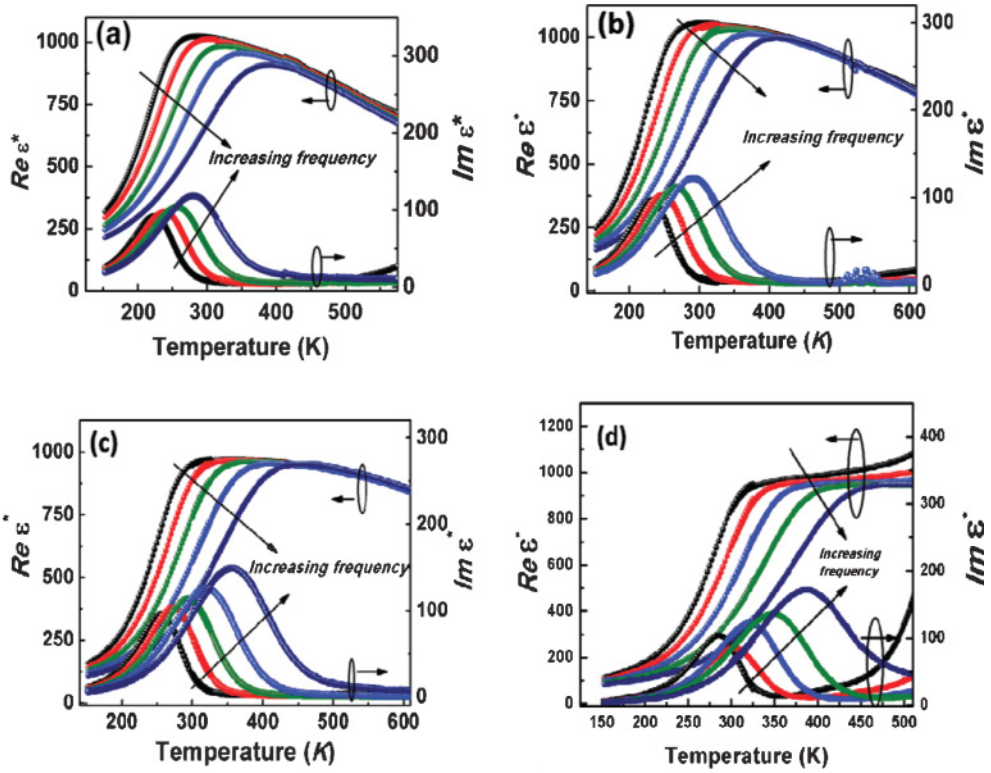

FIG. 2. (Color online) Real and imaginary dielectric permittivity responses as a function of temperature in $(1-x)BaTiO_3$-$xBiScO_3$ ceramics for x values (a) 0.1, (b) 0.2, (c) 0.3, and (d) 0.4. The representative curves are plotted in frequency decades between 100 Hz and 1 MHz.

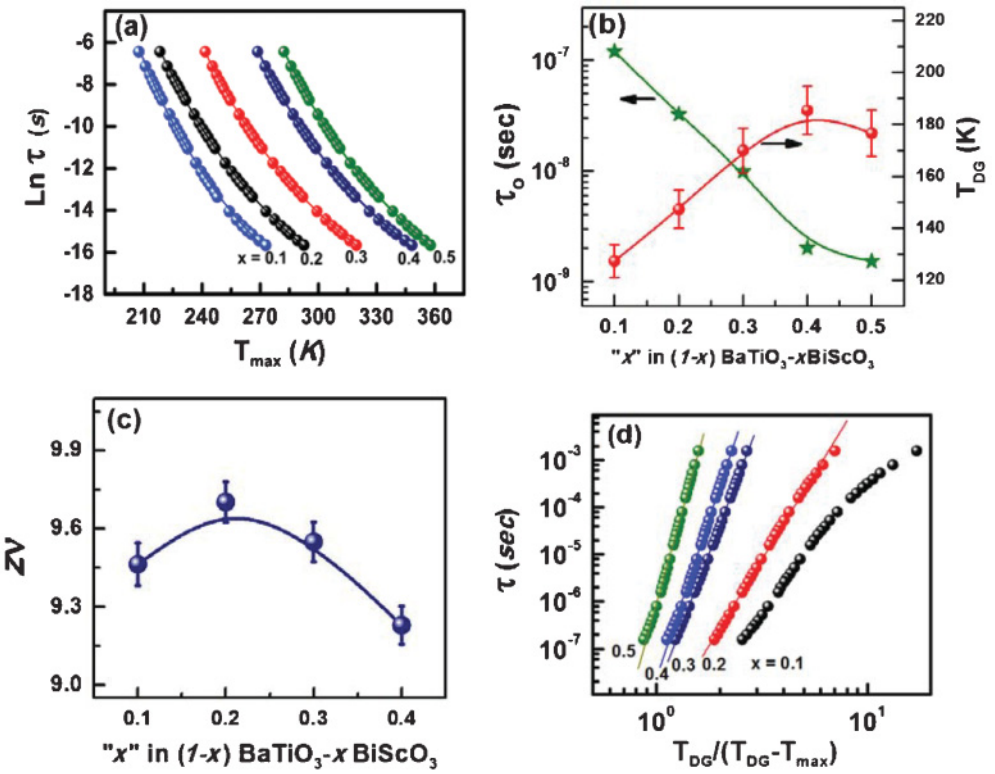

FIG. 3. (Color online) (a) Temperature dependence of the characteristic relaxation time $\tau(T_{max})$, (b) the macroscopic time constants (τ_0) and glass transition temperature (TDG), (c) the scaling exponent ($z\nu$), and (d) the scaling of $\tau(T_{max})$ with $T_{DG}/(T_{DG}-T_{max})$ for $(1-x)BaTiO_3$-$xBiScO_3$ samples with $0.1 \leqslant x \leqslant 0.5$.

$(1-x)BaTiO_3$-$xBiScO_3$ ceramics for x values from 0.1 to 0.4. These measurements were done while cooling the samples at a rate of −3 K/min from 600 K. The samples were held at 675 K for 15 min prior to measuring the dielectric permittivity to minimize history effects. The real part of the permittivity (Re ε^*) was largely independent of frequency above T_{max}, whereas the imaginary part (Im ε^*) exhibited a frequency-dependent peak related to a distribution of relaxation times. As has been reported previously, no dielectric anomalies owing to structural phase transitions were noticed in samples with $0.1 < x < 0.2$, even though recent structural investigations indicate a $T_c \sim 417$ K from mixed rhombohedral and tetragonal phases to a cubic phase for $x \sim 0.15$.[5,13] All the samples exhibited Re $\varepsilon^* \sim 1000$ at 1 kHz at 300 K. These values are comparable to those of previously reported ceramics.[3,5]

Ogihara, Randall, and Trolier-McKinstry[5] analyzed the dielectric relaxation in $(1-x)BaTiO_3$-$xBiScO_3$ samples within the framework of the Vogel-Fulcher law. The reported activation energies were found to be higher than those of relaxor ferroelectrics such as PMN.[34] To understand these intriguing features, the complex dielectric response (Fig. 2) was reanalyzed following critical slowing down dynamics described by[36]

$$\tau_{max} = \tau_0 \left(\frac{T_{max} - T_{DG}}{T_{DG}} \right)^{-z\nu}, \qquad (3)$$

where $z\nu$ is the dynamic exponent, T_{DG} is the dipolar glass transition temperature, T_{max} corresponds to the temperature at which Im ε^* goes through a maximum, and τ_0 is the microscopic relaxation time. In Eq. (3), the critical relaxation time τ_{max} scales with the correlation length ξ as $t_{max} \sim \xi^z$ and the correlation length diverges for $T \to T_{DG}$ as $\xi \sim |T_{max} - T_{DG}|^{\nu}$. As shown in Fig. 3, the peaks observed in Im $\varepsilon^*(T,\omega)$ are better defined than those of Re $\varepsilon^*(T,\omega)$ at all measured frequencies. Therefore, T_{max} was determined from the Im $\varepsilon^*(T,\omega)$ data as shown in Fig. 3(a).

The time constants (τ_0) were found to decrease with increasing $BiScO_3$ concentration from 1.2×10^{-7} s for $x = 0.1$ to 1.5×10^{-9} s for $x = 0.5$, as shown in Fig. 3(b). The τ_0 values are significantly larger than phonon time constants (10^{-12}–10^{-13} s).[3,6] This suggests that the relaxation is governed by dipolar polarizability. The T_{DG} values increased with increasing x. For $x \sim 0.1$, T_{DG} was ~100–120 K, whereas for $x \sim 0.4$ the T_{DG} was ~190–200 K. In addition, the estimated critical exponents ($z\nu$) for $0.1 \leqslant x \leqslant 0.4$ samples [Fig. 3(c)] were between 9.0 and 9.7 with a maximum near $x \sim 0.2$. The calculated critical exponent values correspond reasonably to a three-dimensional (3D) Ising spin-glass model (theoretical value ~10).[24,37] Figure 3(d) depicts the scaling of $\tau(T_{max})$ with respect to the reduced temperature, $T_{DG}/(T_{DG} - T_{max})$. As can be seen, good scaling is obtained for all samples. These results imply that the dipolar clusters within the sample are undergoing critical slowing down phenomena with "weak" or no mutual interactions between the clusters for temperatures below T_{DG}.[38]

Both magnetic spin glasses and dipole glasses exhibit aging, memory, and rejuvenation effects below T_{DG}.[39] *Aging* is a slow

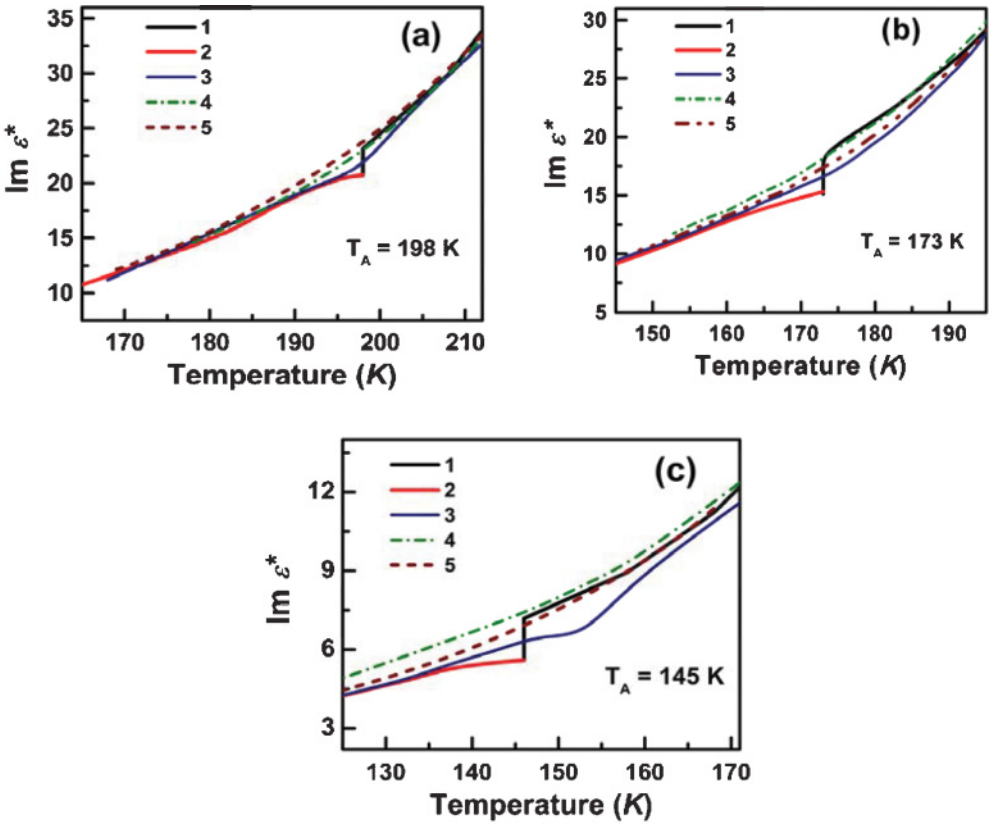

FIG. 4. (Color online) Temperature dependence of Im ε^* measured after aging at (a) $T_A \sim 198$ K, (b) $T_A \sim 173$ K, and (c) $T_A \sim 145$ K. Line 1 was taken during cooling at approximately −10–15 K/min from high temperature to T_A; the sample was aged at T_A for more than 10 h. Lines 2 and 3 are measurements on subsequent cooling and heating cycles (∼3 K/min sweep rates), respectively. Lines 4 and 5 were collected on cooling from 600 K at −2 K/min rate after cycle Nos. 1, 2, and 3.

reduction in the complex permittivity during holds at a constant temperature (T_A) below the glass transition temperature, T_{DG}. If the complex permittivity recovers on further cooling to its original value before aging (i.e., to the value observed on a reference curve measured during continuous cooling) this is known as *rejuvenation*. The net result is that the permittivity versus temperature trace exhibits a dip or hole. On subsequent heating through T_A, ε^* may completely or partially retrace the dip formed during aging; this is called *memory*.

To determine whether comparable behavior would be observed in $(1-x)BaTiO_3$-$xBiScO_3$, samples with $x \sim 0.3$ were chosen. The dielectric permittivity was measured as a function of temperature on cooling with a hold at fixed temperatures (T_A) above and below T_{DG}, as shown in Fig. 4. In the present case, the samples were cooled at a rate of −15 K/min from above 523 K to stopping temperatures of ∼275 K ($\gg T_{DG}$), ∼198 K ($>T_{DG}$), and 173 and 145 K ($<T_{DG}$). The temperature dependence of the permittivity was monitored with a sweep rate of ∼3 K/min as a function of aging time at various T_A's. All of the aging experiments were done with a 1 V_{rms} oscillation at 100 Hz following protocols given elsewhere.[40] After a 10-h holding time, no aging was detected for $T_A > 250$ K. For $T_A < 225$ K, the reduction in dielectric losses was more prominent than the changes in Re ε^*, hence the imaginary part was chosen to illustrate the memory and rejuvenation effects. As shown in Fig. 4(a), for $185 < T_A < 250$ K, cumulative aging develops in the dielectric loss component; however, the aged dielectric losses were rejuvenated almost fully with subsequent cooling and heating cycles. From 185 to 165 K, the dielectric loss exhibited stronger, cumulative aging, with less rejuvenation. For example, for $T_A \sim 173$ K, Im ε^* decreased from 19 to 16 (∼18% reduction). Further sequential cooling→heating→cooling cycles could not completely rejuvenate the Im ε^* to the initial value, as shown in Fig. 4(b)). On the other hand, below T_{DG} ($T_{DG} \sim 170$ K) the samples showed a *cumulative* property change and holelike memory effects, similar to those previously noted in PMN-PT (90/10) relaxor ferroelectrics,[40] as shown in Fig. 4(c)). Holding the $x = 0.3$ sample at $T_A = 145$ K for 10 or 12 h reduced the dielectric losses and further cooling→heating→cooling cycles exhibited memory associated with the thermal history, confirming a classic "hole" aging phenomenon. A noticeable small spread in the holelike memory to slightly higher temperature (up to 155 K) on the temperature scale can been noticed from Fig. 4). Such a small spread in holelike memory on temperature window below glass transition temperature was noticed even in PMN-PT (90/10) single crystals.[33] We believe this spread could be owing to local anisotropic interaction of random fields or temperature measurement artifacts. Thus, in general, the $(1-x)BaTiO_3$-$xBiScO_3$ ceramic samples have typical dipole glass features below T_{DG}. These features indicate

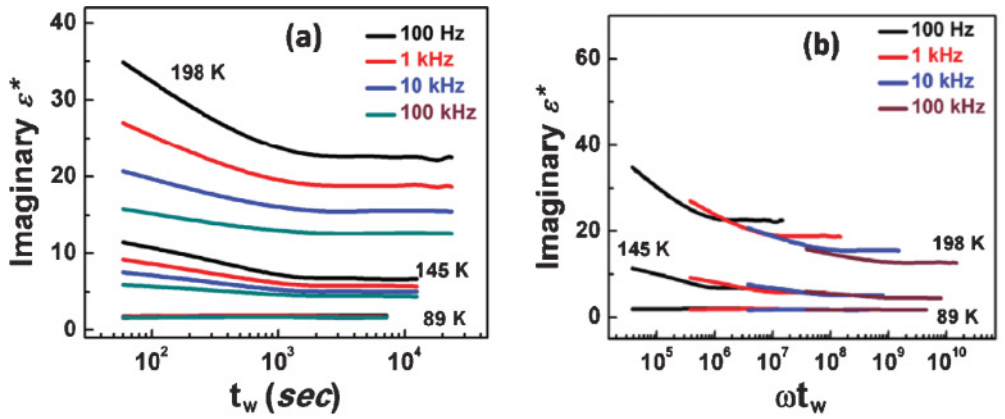

FIG. 5. (Color online) Isothermal aging as monitored via the imaginary part of the dielectric susceptibility in $0.7BaTiO_3$-$0.3BiScO_3$ ceramics for four different frequencies at $T = 198$, 145, and 90 K as a function of (a) wait time (t_w) and (b) angular frequency × wait time (ωt_w). Scaling of Im ε^* with ωt_w below T_{DG} (~150 K) confirms the dipole glass features.

the possibility of collective dynamics and the breakdown of local ergodicity below T_{DG} depending on the thermal history.

A common feature of spin-glass systems is the existence of nonequilibrium dynamics. As a result, aging in dipole glasses depends on the measurement time scale as well as the evolution rate of the nonergodic energy landscape. To investigate this in $(1-x)BaTiO_3$-$xBiScO_3$ ($x = 0.3$), the aging in Im ε^* was determined at a fixed T_A as a function of wait time, t_w, and probing frequency. Figure 5 illustrates the imaginary component of the dielectric permittivity as a function of t_w and ωt_w, respectively. As can be seen, the aging in these samples is explained better by using ωt_w scaling, as the response curves converge over all the measured frequencies below T_{DG}. Im ε^* in these samples scaled as[41]

$$\varepsilon''(\omega,t) = \varepsilon_0''(\omega) + B(\omega t_w)^{-\beta}, \tag{4}$$

where $\varepsilon_0''(\omega) = A\omega^{\alpha}$ is the infinite time "equilibrium" value; β was between 0.12 and 0.17 below T_{DG}. In Eq. (4), the second term may be owing to slow coarsening processes of dipolar clusters during aging below T_{DG}.[28] In dipole glasses, the cumulative part of the aging can be ascribed to slow cluster coarsening in a medium with randomly distributed pinning centers, and is characterized by scaling with ωt_w. Thus, in $(1-x)BaTiO_3$-$xBiScO_3$, the aging is analogous to aging in spin glasses.[40]

In order to evaluate the possibility of reentrant behavior in this system, the temperature-dependent remanent polarization (P_r) and coercive fields (E_c) were measured as shown in Fig. 6. For all compositions, the polarization response is essentially reversible at 300 K. Hysteresis develops at lower temperatures; both the coercive field and the remanent polarization undergo maxima and then drop on decreasing temperature. In addition, the temperatures of the maxima were within ±10 K of either the T_f values obtained from the Vogel-Fulcher expression or the T_{DG} obtained from Eq. (2). The temperature of the maxima in P_r was found to be slightly higher than that of E_c; no thermal hysteresis was detected between measurements on heating and cooling for $0.1 < x < 0.5$. For $x = 0.2$ samples, an anomaly is apparent at ~230 K in the P_r and E_c vs T responses; no corresponding features were seen in the dielectric permittivity versus temperature (Fig. 2). Further, these samples exhibited reentrant polarization independent of the cooling fields, as shown in Fig. 7. As an example, for $x = 0.2$ samples, under field-cooling experiments at 35 and 65 MV/m, as T is lowered, there is an initial increase in the P_r, but on further cooling, P_r dropped again, essentially vanishing at low T. The development of maxima in the switchable polarization appears to be a dielectric analog of the behavior observed in reentrant spin-glass systems, in which a remanent magnetization develops below T_{max} in between the ergodic and the nonergodic spin-glass states.[42,43] In contrast, in relaxor

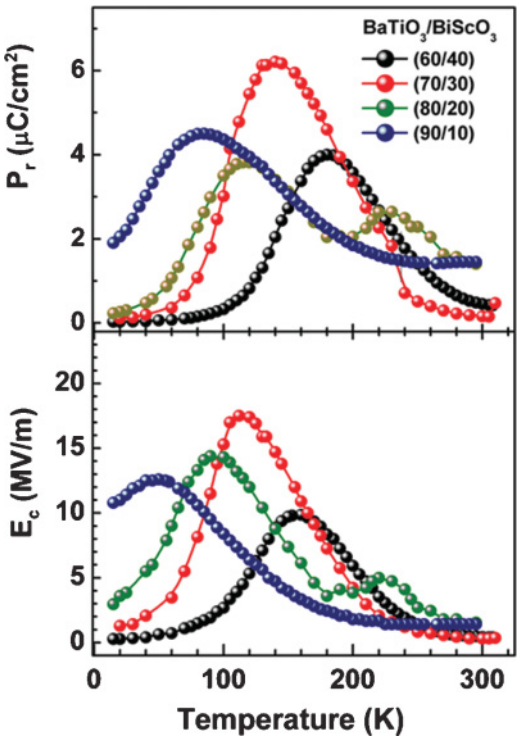

FIG. 6. (Color online) Remanent polarization (P_r) and coercive field (E_c) as a function of temperature in $(1-x)BaTiO_3$-$xBiScO_3$ samples ($0.1 \leqslant x \leqslant 0.4$).

ferroelectrics such as PMN and strontium barium niobate (SBN) P_r and E_c rise as the temperature continues to fall.

For $x = 0.3$ ceramics, thermoremanent polarization measurements were investigated to support the zero-field-cooling aging experimental results. For this purpose, the samples were poled with a ~37 MV/m dc field while cooling from 500 K. At $T > T_{DG}$ and $T < T_{DG}$, the samples were maintained for 15 min before measuring the P_r values from P vs E responses at different time intervals with ~35 MV/m. Figure 8 shows the time decay of the remanent polarization of 0.7 $BaTiO_3$-0.3$BiScO_3$ over $1 < t < 2 \times 10^4$ s at two different temperatures. P_r relaxed in a comparatively short time scale for $T > T_{DG}$. As shown in Fig. 8, ~37% of the original value of P_r relaxed within 2×10^4 s at 193 K $> T_{DG}$. On the other hand, the relaxation times increased for $T < T_{DG}$. The P_r decreased approximately logarithmically with time at 146 K (below T_{DG}). Additional measurements at 80 K (for $\sim 5 \times 10^3$ s) indicated no drop in the remanent polarization with time. The thermoremanent polarization versus time data were fitted by using a stretched exponential relation,

$$P_r(t) = P_0 \exp\left[-\left(\frac{t}{t_p}\right)^{1-n}\right], \tag{5}$$

where P_0, n, and t_p depend upon temperature (T). If $n = 0$, the equation reduces to a single time constant: a Debye-type exponential relaxation. On the other hand, if $n = 1$, the relation converges to a constant value, P_0. For $T = 193$ K ($> T_{DG}$), the estimated P_0, n, and t_p values are (6.5 ± 0.3) $\mu C/cm^2$, 0.78, and 4.2×10^{-5} s, respectively. Good agreement for P_r versus time data was obtained for short time scales; the primary deviations were apparent at longer times, yielding an R^2 value ~0.94 for $T = 193$ K. However, significant deviations from (5) appeared for temperatures below T_{DG} and very poor fits were obtained for P_r versus time data at $T = 143$ K. Thus, we

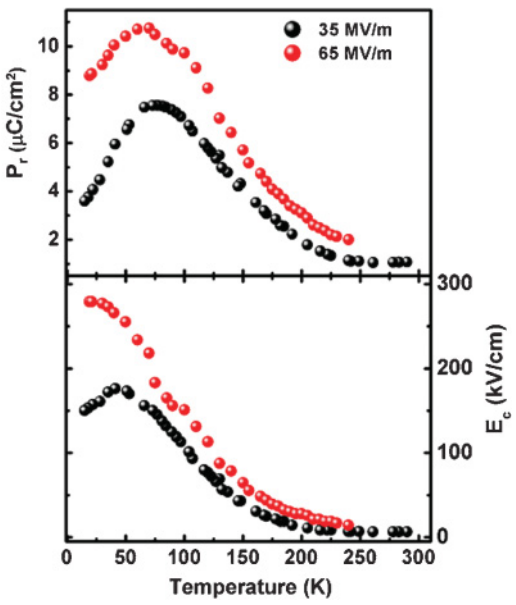

FIG. 7. (Color online) Remanent polarization (P_r) and coercive field (E_c) as a function of field cooling in 0.8$BaTiO_3$-0.2$BiScO_3$ samples. The samples were cooled under fields and the switchable polarization was measured while heating the sample.

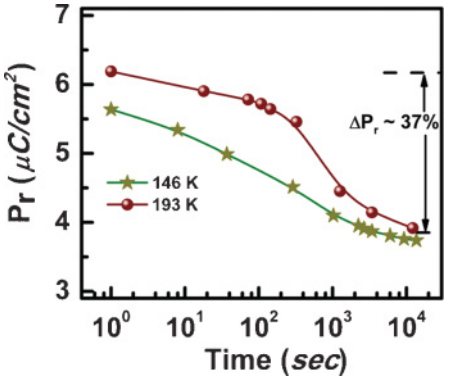

FIG. 8. (Color online) P_r vs time measured at $T = 193$ K ($> T_{DG}$) and $T = 146$ K ($< T_{DG}$).

believe a simple stretched exponential relation is insufficient to describe the polarization freezing in these materials below T_{DG}, presumably owing to the ωt_w relaxation.

Significant differences can be noticed between the behavior of $(1-x)BaTiO_3$-$xBiScO_3$ $(0.1 \leqslant x \leqslant 0.4)$ and canonical relaxor ferroelectrics such as $Pb(Mg_{1/3}Nb_{2/3})O_3$. $Pb(Mg_{1/3}Nb_{2/3})O_3$ single crystals and ceramics show (i) no significant drop in P_r below the glass transition temperature (~223 K) even though they exhibit aging and rejuvenation effects,[44] (ii) relaxation time constants on the order of 10^{-12} s, and (iii) activation energies $\leqslant 0.1$ eV, whereas for $(1-x)BaTiO_3$-$xBiScO_3$ $(0.1 \leqslant x \leqslant 0.4)$, the activation energies are ~0.2–0.3 eV. These results suggest that the dielectric relaxation in $(1-x)BaTiO_3$-$xBiScO_3$ $(0.1 < x < 0.5)$ samples is controlled by frustrated polarization states owing to the formation of weakly interacting polar clusters.

The observed response in these $(1-x)BaTiO_3$-$xBiScO_3$ high energy density dielectrics is in many ways the electrical analog of reentrant magnetic spin-glass systems.[45] In general, the remanent magnetizations in reentrant spin glasses exhibit a maximum at the freezing temperature, before dropping at lower temperatures in the zero-field-cooled case; i.e., the samples develop a more ordered state before going back to a more disordered state at low temperatures. It is possible that competitive dipolar interactions and/or local stresses could be responsible for the reentrant dipole glass features in $(1-x)BaTiO_3$-$xBiScO_3$ for $0.1 < x < 0.5$. In reentrant spin-glass systems, such as $Eu_{1-x}Sr_xS$, the existence of reentrant ferromagnetic features has been established for a critical concentration range (before entering into a pure spin glass state).[28] Recent structural studies indicate that $(1-x)BaTiO_3$-$xBiScO_3$ $(0.1 < x < 0.5)$ is cubic down to 10 K.[5,13] It is possible that substantial local random dipole frustration is responsible for the reentrant ferroelectric state in the macroscopically cubic $(1-x)BaTiO_3$-$xBiScO_3$ $(0.1 < x < 0.5)$ samples.

Based on these arguments, a dielectric phase diagram is proposed as shown in Fig. 9. For $x < 0.05$, the solid solution is ferroelectric below the Curie temperature T_C. Above T_{max} for $0.1 \leqslant x \leqslant 0.4$, the solid solution is cubic and paraelectric. Near T_{DG}, the samples with $0.1 \leqslant x \leqslant 0.4$ show a switchable polarization (shaded region in Fig. 9) before entering into a nonergodic dipole glass state. The maximum P_r is observed close to T_{DG}. To minimize error associated with finite high-field dielectric losses, the shaded region in

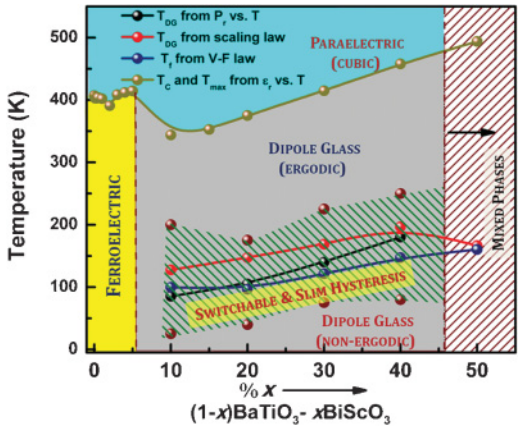

FIG. 9. (Color online) Proposed phase diagram of $(1-x)BaTiO_3$-$xBiScO_3$ ($0.1 < x < 0.5$). Data for Curie temperature (T_C) for $x \leqslant 0.05$ was taken from Ref. 5), and the samples with $0.05 < x < 0.1$ have a core shell structure.

Fig. 9 was assigned where a switchable polarization could be unambiguously detected above the background.

The origin of the reentrant dipole glass behavior is not known in these $(1-x)BaTiO_3$-$xBiScO_3$ ($0.1 < x < 0.5$) samples. One possibility is that it arises from a competition between local ferroelectric and antiferroelectric order. A second potential mechanism could be owing to development of comparatively deep local potential valleys associated with the local polar regimes below T_{DG}. Another, potential mechanism following reentrant magnetic literature is random field–random anisotropy within these samples.[46] These should certainly not be considered an exhaustive list of the possibilities. Further structural studies at low temperatures might be useful in clarifying this point.[14,47] As high temperature–high energy density dielectrics become more important for developing SiC inverter circuits for power electronics, it is clear that understanding the advantages of these polar mechanisms is important to the pure and applied dielectrics community.

IV. SUMMARY

$(1-x)BaTiO_3$-$xBiScO_3$ ($0.1 \leqslant x \leqslant 0.4$) solid solutions have recently emerged as a high energy density capacitor material with energy densities $\sim 6\ J/cm^3$ at room temperature and above. Here it is shown that the dielectric relaxation in $(1-x)BaTiO_3$-$xBiScO_3$ ($0.1 \leqslant x \leqslant 0.4$) solid solutions is consistent with the 3D Ising spin-glass model with critical slowing down characteristics below T_{DG}. T_{DG} increased with increasing $BiScO_3$ composition for $0.1 \leqslant x \leqslant 0.4$. Samples with $0.1 \leqslant x \leqslant 0.4$ exhibited aging, memory, and rejuvenation features similar to dipole glasses. Between T_{max} and T_{DG}, the $(1-x)BaTiO_3$-$xBiScO_3$ ($0.1 \leqslant x \leqslant 0.4$) solid solution behaved as a ferroelectric with finite remanent polarization and coercive fields. Reentrant dipole glass features were confirmed from temperature-dependent polarization studies. A frustrated dipolar glassy phase below T_{DG} developed and is thought to be owing to noninteracting or weakly coupled polar nanoregions. The trends in the data are summarized in the form of a compositional–temperature dielectric phase diagram.

ACKNOWLEDGMENTS

This work was supported by the National Science Foundation, as part of the Center for Dielectric Studies at the Pennsylvania State University, under the Industry/University Cooperative Research Center (I/UCRC) Grant No. 0628817, and by a National Security Science and Engineering Faculty Fellowship.

*bss11@mri.psu.edu

[1] F. C. Lee, J. D. van Wyk, D. Boroyevich, T. Jahns, R. D. Lorenz, T. Paul Chow, R. Gutmann, P. Barbosa, ATKAAF **44**, 5 (2003).
[2] R. J. Kerkman, G. L. Skibinski, and D. W. Schlegel, in *APEC '99–Fourteenth Annual Applied Power Electronics Conference and Exposition* (IEEE, New York, 1999), vol. 1, p. 28.
[3] H. Ogihara, C. A. Randall, and S. Trolier-McKinstry, J. Am. Ceram. Soc. **92**, 110 (2009).
[4] D. S. Tinberg and S. Trolier-McKinstry, J. Appl. Phys. **101**, 024112 (2007).
[5] H. Ogihara, C. A. Randall, and S. Trolier-McKinstry, J. Am. Ceram. Soc. **92**, 1719 (2009).
[6] H. Y. Guo, C. Lei, and Z.-G. Ye, Appl. Phys. Lett. **92**, 172901 (2008).
[7] C.-C. Huang, D. P. Cann, X. Tan, and N. Vittayakorn, J. Appl. Phys. **102**, 044103 (2007).
[8] Z. Yao, H. Liu, Y. Liu, Z. Li, X. Cheng, M. Cao, and H. Hua, J. Ceram. Soc. Jpn **116**, 1150 (2008).
[9] F. Jona and G. Shirane, *Ferroelectric Crystals* (Dover, New York, (1993).
[10] A. A. Belik, S. Iikubo, K. Kodama, N. Igawa, S. Shamoto, M. Maie, T. Nagai, Y. Matsui, S. Y. Stefanovich, B. I. Lazoryak, and E. Takayama-Muromachi, J. Am. Chem. Soc. **128**, 706 (2006).
[11] Y. Y. Tomashpol'skii, E. V. Zubova, K. P. Burdina, and Y. N. Venevtsev, Sov. Phys. Crystallogr. **13**, 859 (1969).
[12] S. Trolier-McKinstry, M. D. Biegalski, J. Wang, A. A. Belik, E. Takayama-Muromachi, and I. Levin, J. Appl. Phys. **104**, 044102 (2008).
[13] K. Datta and P. A. Thomas, J. Appl. Phys. **107**, 043516 (2010).
[14] C. J. Stringer, M. J. Lanagan, T. R. Shrout, and C. A. Randall, Jpn. J. Appl. Phys. **46**, 1090 (2007).
[15] A. Ogielski, Phys. Rev. B **32**, 7384 (1985).
[16] V. V. Shvartsman, S. Bedanta, P. Borisov, and W. Kleemann, Phys. Rev. Lett. **101**, 165704 (2008).
[17] C. A. Randall, A. S. Bhalla, T. R. Shrout, and L. E. Cross, J. Mater. Res. **5**, 829 (1990).
[18] V. Bobnar, Z. Kutnjak, R. Pirc, and A. Levstik, Phys. Rev. B **60**, 6420 (1999).
[19] A. K. Tagantsev and A. E. Glazounov, Phys. Rev. B **57**, 18 (1998).
[20] The term "spin glass" is sometimes used to denote only a "nonergodic" state with infinite relaxation time.
[21] M. Cantoni, S. Bharadwaja, S. Gentil, and N. Setter, J. Appl. Phys. **96**, 3870 (2004).
[22] M. D. Glinchuk and V. A. Stephanovich, J. Appl. Phys. **85**, 1722 (1999).
[23] A. A. Bokov and Z. -G. Ye, J. Mater. Sci. **41**, 3 (2006).

[24]S. F. Edwards and P. W. Anderson, J. Phys. F **5**, 965 (1975).
[25]J. A. Mydosh, in *Spin Glasses–An Experimental Introduction* (Taylor & Francis, London, 1993).
[26]W. Kleemann, J. Non-Cryst. Solids **66**, 207 (2002).
[27]L. E. Cross, Ferroelectrics **76**, 241 (1987).
[28]K. Binder and A. P. Young, Rev. Mod. Phys. **58**, 801 (1986).
[29]E. M. Chudovsky, W. M. Saslow, and R. A. Serota, Phys. Rev. B **33**, 251 (1986).
[30]K. Jonason, J. Mattsson, and P. Nordblad, Phys. Rev. Lett. **77**, 2562 (1992).
[31]T. Sato, T. Ando, T. Ogawa, S. Morimoto, and A. Ito, Phys. Rev. B **64**, 184432 (2001).
[32]V. A. Trepakov, M. E. Savinov, S. A. Prosandeev, S. E. Kapphan, L. Jastrabik, and L. A. Boatner, Phys. Status Solidi C **2**, 145 (2005).
[33]E. V. Colla, P. Griffin, M. Delgado, M. B. Weissman, X. Long, and Z. G. Ye, Phys. Rev. B **78**, 054103 (2008).
[34]D. Viehland, S. J. Jang, L. E. Cross, and M. Wuttig, J. Appl. Phys. **68**, 2916 (1990).
[35]U. T. Hoechli, K. Knorr, and A. Loidl, Adv. Phys. **39**, 405 (1990).
[36]D. S. Fisher, Phys. Rev. Lett. **56**, 416 (1986).
[37]K. Gunnarsson, P. Svedlindh, P. Nordblad, L. Lundgren, H. Aruga, and A. Ito, Phys. Rev. Lett. **61**, 754 (1988).
[38]Z. Slanič, D. P. Belanger, and J.-A. Fernandez-Baca, Phys. Rev. Lett. **82**, 426 (1999).
[39]W. Kleemann, J. Dec, P. Lehnen, R. Blinc, B. Zalar, and R. Pankrath, Europhys. Lett. **57**, 14 (2002).
[40]L. K. Chao, E. V. Colla, and M. B. Weissman, Phys. Rev. B **74**, 014105 (2006).
[41]*Spin Glasses and Random Fields*, Vol. 12 of *Series on Directions in Condensed Matter Physics*, edited by A. P. Young (World Scientific, Singapore, 1998).
[42]K. Jonason and P. Nordblad, Eur. Phys. J. B **10**, 23 (1999).
[43]M. A. Manheimer, S. M. Bhagat, and H. S. Chen, J. Magn. Magn. Mater. **38**, 147 (1983).
[44]E. V. Colla, L. K. Chao, M. B. Weissman, and D. D. Viehland, Phys. Rev. Lett. **85**, 3033 (2000).
[45]J. Mattsson, T. Jonsson, P. Nordblad, H. A. Katori, and A. Ito, Phys. Rev. Lett. **74**, 4305 (1995).
[46]S. Abiko, S. Niiddera, and F. Matsubara, Phys. Rev. Lett. **94**, 227202 (2005).
[47]S. Jesse, B. J. Rodriguez, A. P. Baddorf, I. Vrejoiu, D. Hesse, M. Alexe, E. A. Eliseev, A. N. Morozovska, and S. V. Kalinin, Nat. Mater. **7**, 209 (2008).